IEEE Access
Multidisciplinary | Rapid Review | Open Access Journal

Received January 30, 2019, accepted March 4, 2019, date of publication May 6, 2019, date of current version July 16, 2019.

Digital Object Identifier 10.1109/ACCESS.2019.2910822

A Technique for MIMO Antenna Design With Flexible Element Number and Pattern Diversity

YASIN KABIRI[1], ALEJANDRO L. BORJA[2], (Member, IEEE), JAMES R. KELLY[3], (Member, IEEE), AND PEI XIAO[4], (Senior Member, IEEE)

[1]5G Innovation Centre, University of Surrey, Guildford GU2 7XH, U.K.
[2]University of Castilla-La Mancha, 02071 Albacete, Spain
[3]Institute for Communication Systems, University of Surrey, Guildford GU2 7XH, U.K.
[4]Faculty of Engineering and Physical Sciences, University of Surrey, Guildford GU2 7XH, U.K.

Corresponding author: Yasin Kabiri (y.kabiri@surrey.ac.uk)

This work was supported by the Engineering and Physical Science Research Council (EPSRC) under Grant EP/N020391/1.

ABSTRACT This paper presents a new technique for designing multiple-input multiple-output (MIMO) antennas having pattern diversity. Massive MIMO is expected to form a part of 5G communications and will require antennas having a very large number of elements. However, due to the size limitation, it is highly challenging to preserve high isolation between the ports. Pattern diversity technique is also highly desirable and can facilitate MIMO systems with diversity gain. However, achieving that within a compact antenna, where there is limited space between the elements, is also challenging. In this paper, a technique is introduced and applied to four- and six-element MIMO antennas. This technique can improve the isolation between the ports, and it also yields pattern diversity for MIMO antennas with various numbers of elements. The technique is verified via the experimental measurement.

INDEX TERMS MIMO antenna, pattern diversity, isolation reduction.

I. INTRODUCTION

Cellular communications was established with the advent of (1G) analog frequency modulation (FM)-based systems in the 1980s. The first 4G network was launched in Stockholm Sweden in 2009. It is expected that 5G networks will be launched around 2020. Utilizing multi-input multiple-output (MIMO) systems, provides an increase in channel capacity without the need for extra radio frequency spectrum or power at the transmitter. Considering the power and bandwidth constrains in the current generation of cellular systems, MIMO techniques offer several advantages including: enhanced bit rate, reduced multipath effects, and increased capacity [1].

The main idea in MIMO systems is to form parallel resolvable channels in order to transmit/receive uncorrelated signals and increase channel capacity. The main challenges in MIMO antenna design include preserving compact size, high radiation efficiency, low envelope correlation, and high port to-port isolation [2]. Achieving such a design would be highly challenging due to the trade-offs which exist between the named features. Many approaches have been proposed to address these challenge as reported in [1]–[16].

The unwanted coupling between the radiating elements in a MIMO system can severely increase signal correlation and decrease radiation efficiency. One approach to address this problem is to exploit pattern diversity to realize uncorrelated channel.

This also adds extra degrees of freedom to the MIMO system diversity gain [14]. A planar Inverted F-antenna is one of the most attractive antenna types for use within a multi-element antenna designs due to its: compact size, low complexity, easy matching, and easy integration with mobile handsets [17].

In [18], [19] a two element IFA was proposed that yields isolation better than 20 dB and 15 dB. However, the antenna elements are not printed on the same pcb. The radiation patterns of the two antenna elements are roughly the same. In [20] a four element planar antenna is proposed. However, that antenna configuration can only achieve −11 dB of port-to-port isolation. To improve the isolation in a MIMO antenna one approach is to use antenna elements that support

The associate editor coordinating the review of this manuscript and approving it for publication was Xiu Yin Zhang.

orthogonal eigenmodes. Although the port-to-port coupling can be reduced effectively via this approach, the use of different elements types will result in different gain and radiation patterns which will degrade the consistency of the performance over the entire angle range [21], [22]. Orthogonally locating the antenna elements to form orthogonal eigenmodes in a MIMO system is another approach is commonly used to reduce the mutual coupling. This approach will be more effective in a MIMO system antenna having a directive radiation pattern [11], [12], [15], [17], [23]. However the limitation with this approach is that good isolation can be achieved for two orthogonal component or when more elements are introduced in the system. However, good isolation cannot be preserved any more. On the other hand in the Massive MIMO concept which is an indispensable part of 5G communication systems, larger numbers of antennas are highly desirable for creation of finer and more directive beams [24].

This paper proposes a technique that can address current requirements for wireless systems and challenges in MIMO antenna design. The proposed technique allows multiple antennas to be collocated on a common ground plane. The technique allows direct and independent control of the gain of antenna element and number of elements in a MIMO system. Regardless of the number of antenna elements in the MIMO system, the proposed technique can guarantee port-to-port isolation better than 20 dB. Depending on the application requirements the gain of the antenna can be controlled by the size of the shared ground plane between the MIMO elements. Therefore it can be used for numerous applications where pattern diversity is a key factor.

Furthermore, the proposed technique targets the need for 5G beam steerable antennas. The elements are located such that they can steer a directive beam from 0-360deg in azimuth. When all ports are excited it forms semi-omnidirectional pattern which could be used for transmission and sensing/searching proposes. To further increase the gain the MIMO antenna can be arrayed.

II. ANTENNA CONCEPT AND DESIGN

A. SINGLE ELEMENT IFA

The structure is low profile with moderate bandwidth and omnidirectional radiation pattern. It is also a good candidate for MIMO purposes as it is robust against unwanted effects from nearby elements. The IFA antenna offers the benefits of compact dimensions, easy integration with active devices and good radiation performance. It is widely used in wireless and mobile communication [14], [23], [25]–[27].

Design procedure: Fig. 1 illustrates the configuration of a single element IFA antenna. The design consists of a wire which is bent in to an L-shape. A feed is introduced to form an F-shape structure, as the name denotes.

Consider Fig. 1, the resonance frequency is set by the distance of the feeding port to the open end of the monopole which is shown here in as L_3. Once the desired operating frequency is set by L_3 then the distance between the feeding port

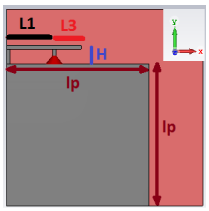

FIGURE 1. The geometry of the single element antenna.

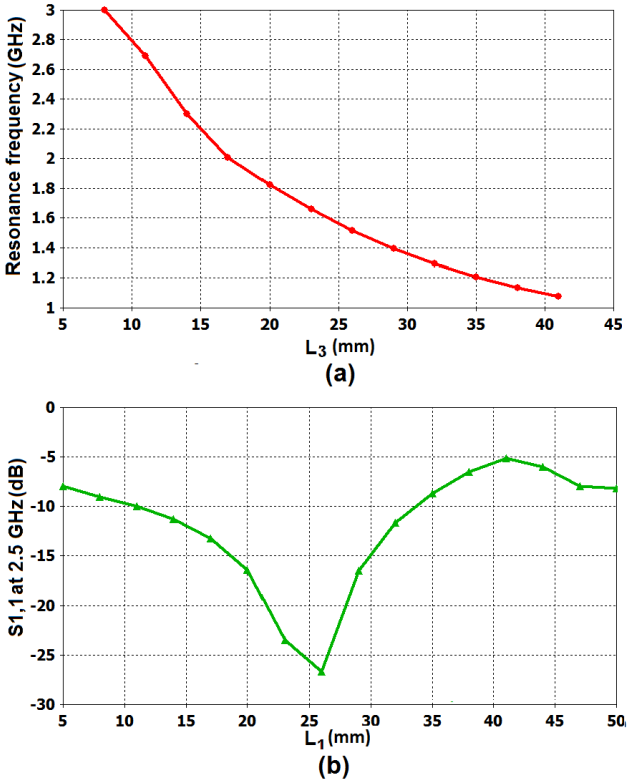

FIGURE 2. (a) The resonance frequency versus L_3 (b) The S11 versus L_1 at spot frequency.

and the shorted end (L_1) can be used to tune the impedance in order to achieve a good matching at the resonance frequency set by the value of L_3. Fig. 2(a) illustrates the effect of the change of parameter L_3 on the resonance frequency. The resonance frequency is decreased as the value of L_3 increases. Therefore, Fig. 2(a) can be used to as starting point for the design to set by the value of L_3 for the desired resonance frequency. Fig. 2(b) illustrates the effect of the L_1 on the matching (S11) at a spot frequency. It illustrates that the parameter L_1 can be used to tune the impedance at the frequency of interest previously by parameter L_3.

Another important parameter in this design is the length of the ground plane (lp) of the illustrated IFA in Fig. 1. This parameter can be used to control the directivity of the main lobe of the antenna. Fig. 3 illustrates the directivity of the single element IFA antenna at the resonant frequency of 2 GHz for different values of lp while other parameters were kept constant. The return loss remains below −15dB for all the values of lp presented in Fig. 3. The position of the antenna is

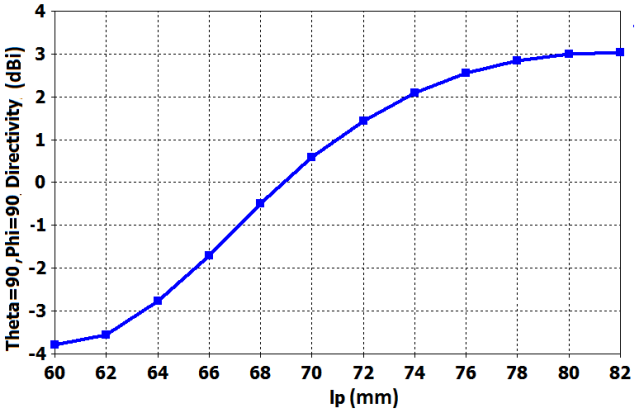

FIGURE 3. Directivity versus the size of the ground plane Lp.

also kept constant at the edge of the ground plane. As Fig. 3 illustrates, the directivity of the single element antenna can be increase (at theta = 90, phi = 90) by increasing lp. This effect will be beneficial in array design, where high directivity in specific direction is highly desired.

B. MIMO IFA

After optimizing and designing the single element antenna, for MIMO operation, it is vital to locate other elements such that they preserve low coupling in order to maximize the diversity performance. It is known in the literature that for an element spacing larger than half of the operating wavelength, low signal correlation can be achieved. In this paper we introduce an approach that ensures low coupling between any number of IFAs on a common ground plane. The limited available space in a shared ground plane, encourages us to exploit three techniques to maximize the diversity performance:

- T-slots: are employed between the radiating IFA elements in order to minimize the coupling between adjacent elements. This allows those radiating elements to be positioned closer than half-a-wavelength on a shared ground plane. The T-slots are aligned along lines of symmetry which bisect the ground plane.
- Pattern diversity: The size of the ground plane can be used to tune the directivity of each radiating element thus minimize the envelope correlation coefficient.
- $2\pi/n$ angular positioning: A common approach for minimizing coupling between the radiating elements of a MIMO antenna is to position the elements orthogonally, as mentioned earlier. In this paper we present a more general approach whereby the relative angle between radiating elements is set to $2\pi/n$ where: n is the number of radiating elements.

In order to validate the developed approach antennas based on 4 elements and 6 elements, were designed, fabricated, and experimentally measured. Fig. 4 illustrates the geometry of the 4 element antenna. The dimensions of the antenna are given in Table 1. This antenna was designed for operation within the LTE-10 band. For this reason the antenna's

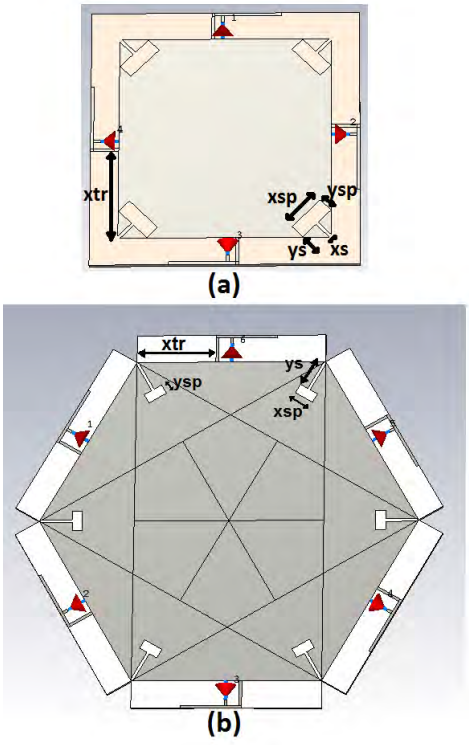

FIGURE 4. The geometry of the 4 and 6 element MIMO antenna. The parameters used in the slot designs are illustrated in Fig. 4 (a). Same parameters are also used in 6 element MIMO.

TABLE 1. Parameters value for 4 and 6-element MIMO antenna in (millimeters).

Parameter	4-element	6-element
L_1	3	5.4
L_3	19.1	16.7
H	9	9
lp	70	70
xsp	6.5	7.3
ysp	5	3.6
xs	1	1
ys	6.7	12
xtr	29.5	29.5

center frequency and 10 dB return loss bandwidth were set to 2.11 GHz and 100 MHz, respectively. The T-slots are chosen such that the directivity is maximized while an isolation of better than 20 dB is preserved. This was achieved using the design procedure outlined below. The antenna is fabricated on an FR4 substrate having a thickness of 1.6 mm, permittivity of 4.3, and loss tangent of 0.025.

The text below provides guidelines that can be used to design the MIMO antenna for a particular application.

1) Setting the IFA element sizes: The desired operating frequency, bandwidth and directivity can be achieved by following the design guidelines for the single element IFA.
2) Setting the number of antenna elements and ground plane configuration: Depending on the number of antenna elements required for the MIMO system,

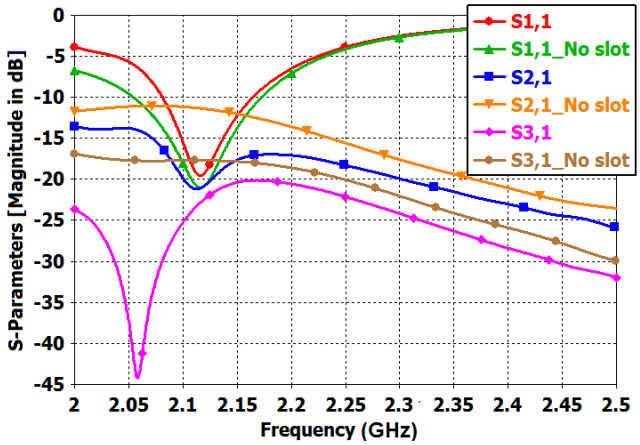

FIGURE 5. The S-parameter of the 4 element MIMO antenna.

the shape of the common ground plane can be set. The number of the sides on the ground plane is equal to the number of antenna elements. For instance for a 4, 5, or 6 element MIMO antenna the ground plane will be square, pentagonal, or hexagonal, respectively.

3) Placing the IFA elements: The positions of the IFAs should now be optimized to minimize the coupling between the elements. A careful parametric study was undertaken which reveals that best isolation is obtained when the IFA elements are placed close to center of their respective sides of the ground plane. If the ground plane dimensions are chosen such that the distance between adjacent elements is larger than half of a wavelength, 20 dB of isolation between elements may be achievable. If this cannot be met, step 4 can be followed.
4) Add T-slots: To improve the isolation between the adjacent ports, T-slots can be placed in the ground plane as explained above.
5) Increase directivity of elements: In order to reduce the envelope correlation coefficient and/or to achieve the directivity required for a specified application, the size of the ground plane can use to tune the pattern. If higher directivity is required, the MIMO system can be arrayed which will be discussed in the array section.

III. RESULTS

A. 4 ELEMENT MIMO ANTENNA

Fig. 5 shows the comparison between measured and simulated scattering parameters for the 4 element MIMO antenna. From Fig. 5 it is clear that a port-to-port isolation in excess of 22 dB was achieved by properly choosing the dimensions of the T-slots. It also shows the S-parameter before and after embedding the T-slot. From these results we can concluded that the addition of the T-slots improves the isolation, between radiating elements, by 11 dB.

The final dimensions of the design are illustrated in Fig. 4(a). Fig. 5 shows the S-parameters of the 4 element MIMO antenna after optimization. From the S11 curve,

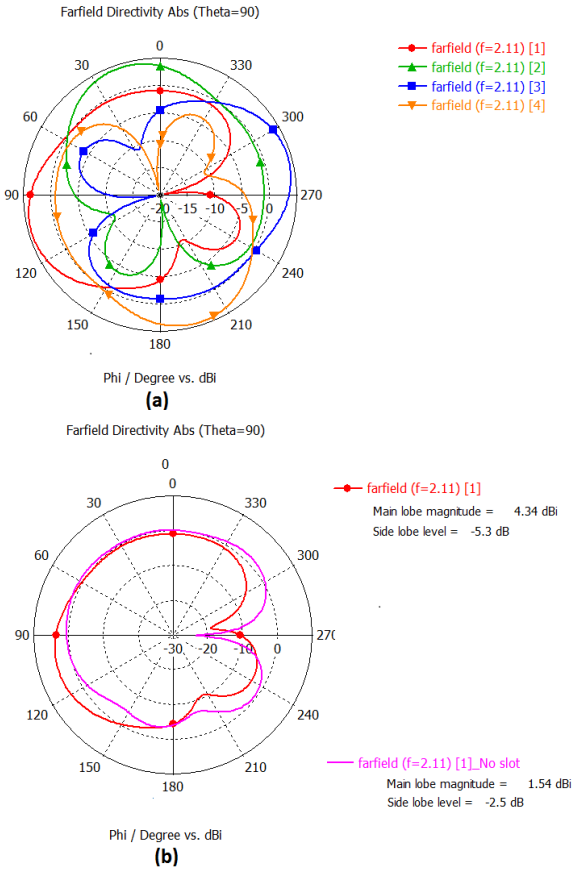

FIGURE 6. Farfield directivity (theta = 90) (a) for all ports of the 4 element MIMO (b) with and without T-slot.

in Fig. 5, it can be seen that there is a resonance at 2.11 GHz. The IFA was designed using the guideline presented in previous section. The designed resonance frequency was achieved by properly choosing the value of L_3. The 10 dB return loss bandwidth was set to 100 MHz by properly choosing the value of L_1. It should be noted that for other desired applications, the values of L_1 and L_3 can be chosen accordingly.

Isolation improvement: A port-to-port isolation better that 22 dB was achieved as illustrated in Fig. 5 (S21 and S31 are below -22dB). The coupling reduction is mainly achieve by properly choosing the dimensions of the T-slots.

Fig. 6 (a) illustrates the radiation pattern of the 4 element MIMO antenna. It shows the patterns associated with all 4 ports. Fig. 6 (b) illustrates the radiation patterns with and without presence of the T-slots in order to highlight their contribution to improving the directivity. From Fig. 6 it can be concluded that the addition of the T-slots improves the main lobe directivity by 2.8 dBi.

The diversity performance of the final 4-element MIMO antenna is illustrated by the Envelope Correlation Coefficient (ECC) in Fig. 7. ECC is a measure to show how correlated two different antennas' radiation patterns are. The ECC varies between 0 and 1 where EEC $= 1$ for two completely identical patterns while for completely independent patterns, the ECC would be 0. For a 4-element MIMO antenna there are

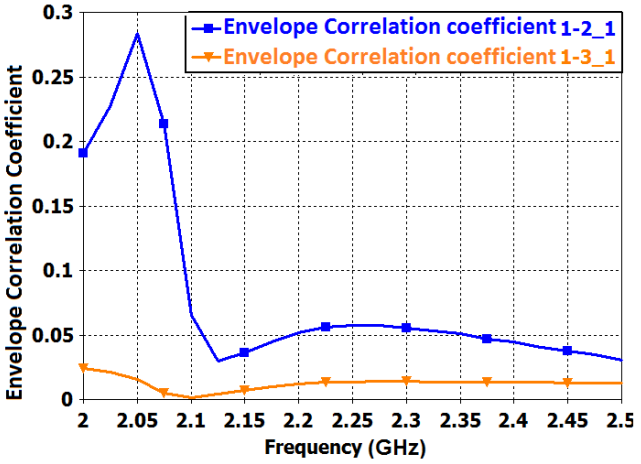

FIGURE 7. All possible combination of envelope correlation coefficient for the 4 elements MIMO antenna.

two main ECCs, namely those associated with the coupling between ports 1 and 2, as well as ports 1 and 3. These ECC are plotted in Fig. 7. The maximum value of the EEC, corresponds to the antenna's resonance frequency of 2.11 GHz, and lies below 0.05. This indicates that the patterns are highly uncorrelated. The directional pattern of the elements (with 90 degree difference between the main lobe angle) and thus very small value of ECC make this antenna a great candidate for pattern diversity in MIMO applications.

B. 6 ELEMENT MIMO ANTENNA

The next example is a 6-element IFA antenna as illustrated in Fig. 4(b). This antenna is designed for operation at a different frequency (2.25GHz) band compared with previous example in order to show the versatility of the design procedure given in the design section of this section. The antenna is fabricated on the FR4 1.6 mm and the final dimensions of the design are illustrated in Fig. 4.

Fig. 9 illustrates the S-parameters for the 6 element MIMO antenna after optimization. The center frequency is set to be 2.25 GHz as illustrated by the S66. The desired center frequency and band width are achieved by following the same design procedure as employed for the 4-elements MIMO antenna. For other desired applications, the values of L_1 and L_3 can be chosen accordingly.

Isolation improvement: Port-to-port isolation better than 24 dB was achieved as illustrated in Fig. 9 (S56, S46, and S36 are all below −24dB). The coupling reduction is mainly attributed to the proper choice of the T-slots dimensions. Fig. 8 illustrates the effect of altering the configuration and dimensions of the slot (illustrated in Fig. 4) on the S16 (i.e. coupling between adjacent ports) as well as the directivity of the 6 elements MIMO antenna. In these figures, the directivity (single port) and isolation of the MIMO antenna are calculated for different combinations of slot size where the X-axis shows xsp values in mm and each curve represents a different values of ys in mm. For a given value of ys, there is a value for xsp that lead to the minimum coupling between the

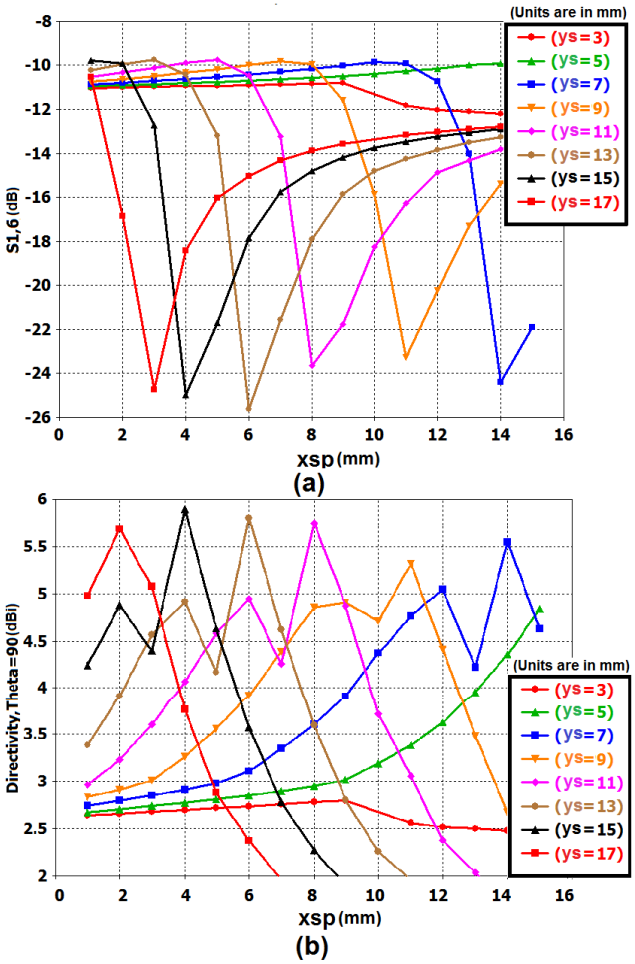

FIGURE 8. T-slot parametric study.

adjacent ports. Also, by comparing Fig. 8(a) and Fig. 8(b) it can be concluded that for slot dimensions where the coupling is minimum between the adjacent ports, the directivity is maximum. On the other hand, different slot dimensions lead to different directivity values and therefore they can be used as a controlling factor. For this example and the chosen size of the ground plane, the minimum coupling and highest value of the directivity was achieved for xsp + ys = 19mm. This value (xsp + ys) depends on the size of the ground plane.

In order to further illustrate the effect of the slots, Fig. 9 illustrates the s-parameters before embedding the T-slots. By comparing the S-parameters of 6-port MIMO antenna with and without the T-slot, it can be concluded that the isolation, between adjacent elements and front to front elements, is improved by at least 13dB.

Radiation pattern improvement: Fig. 10 (a) illustrates the radiation pattern of the 6 element MIMO antenna. The T-slots are dimensioned in order to maximize the directivity while preserving also better than 23 dB of isolation.

This approach yields 6 radiation patterns each pattern has a directivity of 4.28 dBi. The main beam direction of adjacent patterns are separated by an angle of 60deg. The array can thus cover 360deg with a beam crossover value of 4.28 dBi.

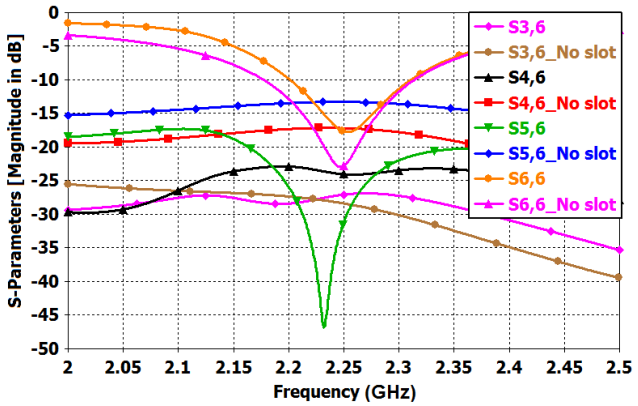

FIGURE 9. The S-parameter of the 6 element MIMO antenna.

In order to show the how the T-slots contribute to improving the radiation pattern, for a given antenna size, the E-field patterns of the antenna for the 6-element MIMO are illustrated with and without presence of the T-slots. This is illustrated in Fig. 6 (b). From this figure it can be concluded that the main beam gain is improved by 3.0 dBi only by adding T-slots.

Diversity performance: To illustrate the diversity performance of the final 6-element MIMO design, Fig. 11 plots the Envelope Correlation Coefficient (ECC). The 6-element MIMO antenna can produce three different combination of patterns. For this reason three ECC curves are illustrated in Fig. 11. The maximum ECC value at the resonant frequency of 2.24 GHz, is not more than 0.01 which proves that the radiation patterns are close to being completely independent. The directional pattern of the elements (with 60 degree difference between the main lobe angles) and the very small value of the ECC make this antenna a great candidate for pattern diversity MIMO application.

C. PARAMETRIC STUDY OF THE MIMO

The position of the ports and the IFA can affect the main lobe direction. For this reason Fig. 12 shows how the main lobe direction of the design can be tuned for different applications. This is illustrated in Fig. 12 for both 4 and 6-elements MIMO antenna. The ports are aligned with y-axis and therefore the reference in this figure is 90 degree. For the 4-element MIMO as the ports moves from edge towards the center of each side of the ground plane, the main lobe direction starts to deviates from 90 degrees. The same effect is also happens for the 6 element MIMO antenna where the main lobe starts to deviate from 85 degree. This graph can be used for the applications where the main lobe direction needs to be set accurately. It should be noted that acceptable impedance matching is preserved as the position of the ports are swept through the range given in Fig. 12.

The T-slot approach can be used to reduce the coupling between the adjacent elements. Based on our simulation based studies we conclude that this approach can guarantee good isolation between the ports (S21 better than −15 dB) provided that the relative distance between the ports is larger

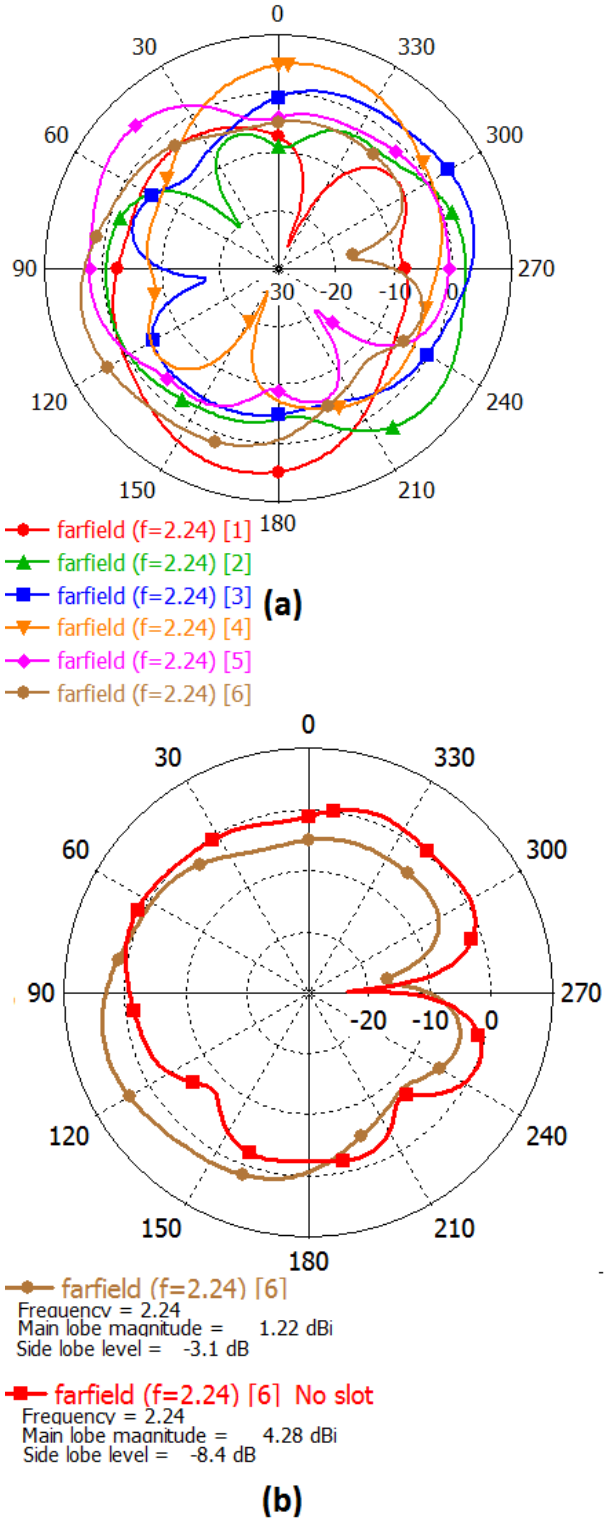

FIGURE 10. Farfield directivity (theta = 90) (a) for all ports of the 6 element MIMO (b) with and without T-slot.

than lambda/4. This therefore places an upper limit on the largest number of elements that can be located within a ground plane of a given size. For a give number of elements, increasing the size of the ground plane will increase the directivity, as illustrated in Fig. 12.

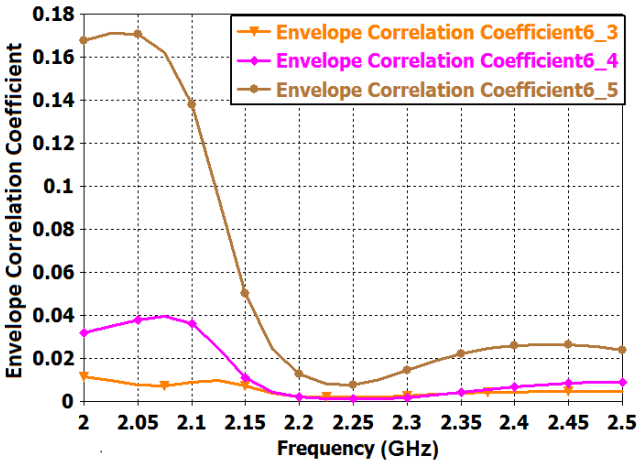

FIGURE 11. All possible combination of envelope correlation coefficient for the 6 elements MIMO antenna.

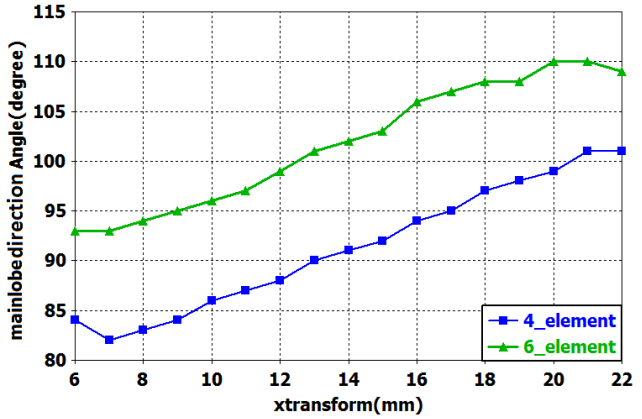

FIGURE 12. The main lobe direction of the antenna VS. the position of the port. The 0 mm is when the antenna is at the edge of the side.

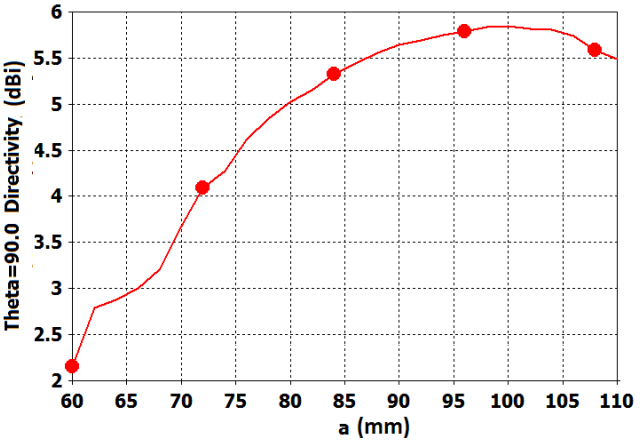

FIGURE 13. The directivity vs. the geometry (a) of the 6 elements MIMO antenna.

Main lobe directivity: The directivity and half power beam width, are important factors in many applications. This design configuration is flexible in terms of the number of antenna elements and facilitates control over directivity and half-power beam width. To allow the MIMO antenna to have the full space coverage (360 degree), the half power beam width for each of antenna elements should be set to 360/n; where n is the number of antenna elements. Fig. 13 illustrates the directivity versus parameter a (the side length of the ground plane). This graph shows that the parameter a can be used to set the required directivity for a given design. The directivity increase as a increase. This graph can be used to design a 6 element MIMO antenna exhibiting a particular directivity. The graph shows that the directivity attains its maximum value when a = 95mm.

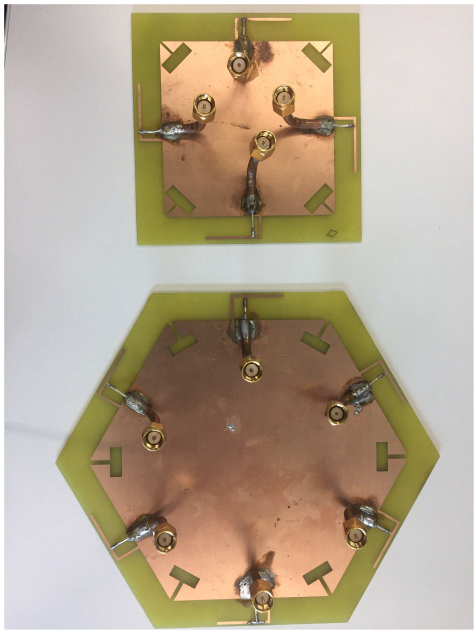

FIGURE 14. The geometry of the fabricated 4 and 6 elements MIMO antenna.

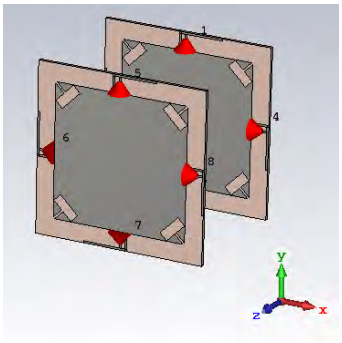

FIGURE 15. The geometry of the array configuration for 4 elements MIMO antenna.

Fig. 14 illustrates the fabricated 4 and 6 element MIMO antennas. To feed the antenna in practice, semi-rigid cable is used. One end of the cable is connected to the SMA connector and the other end is connected to the IFA.

D. ARRAY PERFORMANCE

In some application, such as beam forming, high directivity is desired. To address this need the performance of the proposed technique is illustrated when arrayed. This is illustrated for the 4-element antenna. Two copies of the antenna are

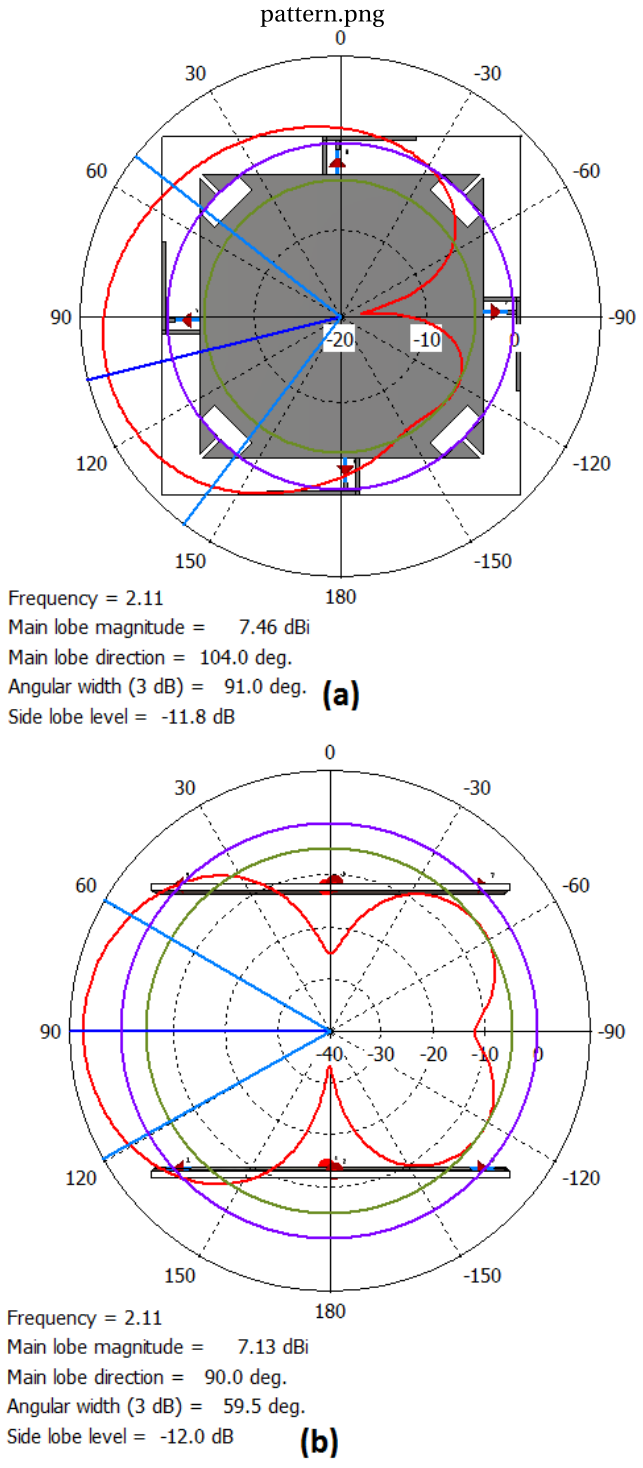

FIGURE 16. The Farfield directivity for four element antenna (a) Theta = 90 (b) Phi = 90 E and H plane of the array 4 elements antenna.

arrayed along the z-axis. The antennas are separated by $\lambda/2$. The configuration of the design is illustrated in Fig 15.

Fig. 16 shows the radiation patterns of the MIMO antenna shown in Fig. 15. The main lobe directivity of the structure is 3.1dBi higher than that of the antenna shown in Fig. 4 (a).

Moreover, the half power beam width (at Theta = 90) is 91 degree which makes it suitable for a 4-element MIMO

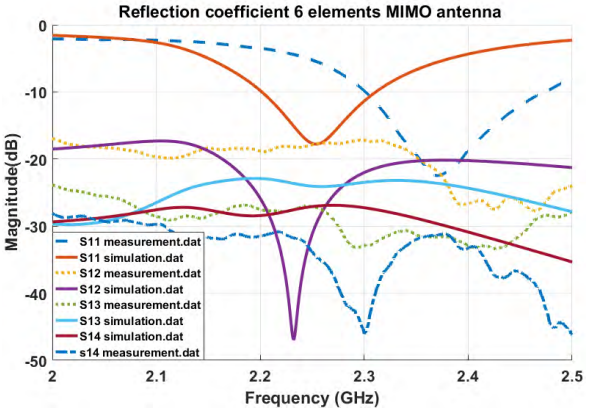

FIGURE 17. The measured and simulated s-parameter of the 6 elements MIMO antenna.

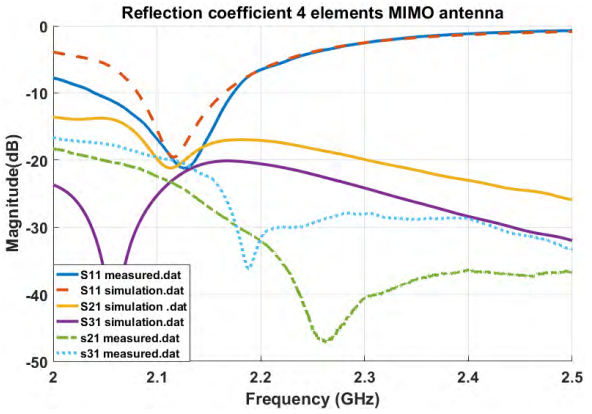

FIGURE 18. The measured and simulated s-parameter of the 4 elements MIMO antenna.

antenna as it can covers full 360 degree using only 4 patterns. The main lobe angle can also be shifted toward 90 degrees by using the Fig. 17. Ports 1 and 5 in the 4 elements MIMO antenna are excited with in-phase signals. This antenna in array configuration will be a great candidate for beam forming applications. This design configuration provides versatility depending the application requirements. The granularity of the number of beams in the elevation plane can be adjusted by varying the number of array elements along the z- axis while the granularity in the azimuth plane can be adjust by varying the number of MIMO elements. When all ports of the proposed configuration are excited simultaneously, the system can be used to search the whole 360 degree. This is useful in some beam-forming application where the system needs to monitor the environment and determines the direction of arrival before establishing the connection for maximizing the capacity of the link.

E. MEASUREMENT

To validate the antenna design and the developed approach, the described 4 and 6 element MIMO antennas were fabricated and measured. To prove the credibility of the simulation, Fig. 17 and Fig. 18 are provided which illustrate the s-parameters for the 4 and 6 element MIMO

TABLE 2. Performance comparison of the proposed approach and reference multiport MIMO antennas.

Ref	technique	number of port	bandwidth (%)	pattern	additional components	min isolation level (dB)	diversity Gain	ECC	Efficiency (%)
[28]	inter digital capacitor	3	3	omnidirectional and broadside	feeding network	20	0.99	0.08	48
[29]	characteristic mode analysis	3	6	omnidirectional and broadside	mode decoupling network	20	0.99	0.04	51.17
[30]	vertically polorised ports	2	4	broadside	power splitters network	35	-	-	-
[31]	printed parasitic reflector	4	12	directional endfire	reconfigurable feeding network	28	-	-	81
[32]	interconnected ground	4	58.6	broadside directional	No	11	-	<0.1	95
[33]	cross-shaped decoupling structure	4	1.6	broadside directional	shorted cross-shaped metal strips	18	0.99	0.08	63
[34]	decoupling structure in ground plane	2	149	omnidirectional	L-shaped strips in the Ground plane	22	9.98	0.01	75
[35]	monopole and patch combination	3	13	endfire and broadside	No	15	9.9	0.008	55
[36]	characteristic modes anlysis	2	130	omnidirectional	No	20	9.9	0.003	70
Prop -osed	T-slot analysis	flexible	20	omnidirectional and directional	T-slot	24	9.9	0.02	75

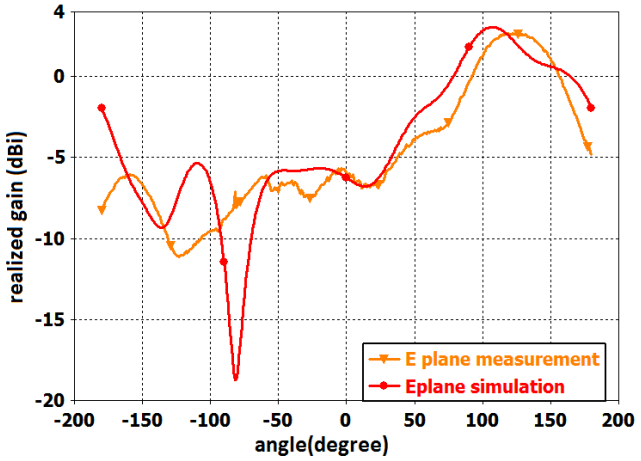

FIGURE 19. The measured and simulated E-field of the 6 elements MIMO antenna.

antenna respectively. The simulated and measured data are in a good agreement and port-to-port isolations better than 20 dB are achieved for both antennas. This validates the developed configuration.

A frequency change (of about 4%) between the simulated and measured results is occurred as it can be seen in Fig.17. This can be arisen form the dielectric and thickness accuracy of FR-4 material. Moreover, to perform measurement of the fabricated antenna, semi rigid cable is used and bended. As this bend is performed manually and not with the most accurate equipment, degrees of impedance mismatch might be arisen from this action. In order to prevent this frequency change, a substrate with more accurate dielectric tolerance such as Roggers 5880 can be used. Also smoother cables or SMA jack (90 degree SMA) can be used to prevent the inaccurate bend.

Moreover, to illustrate the credibility of the radiation patterns in simulation, the measured and simulated E-plane of the 6 elements MIMO antenna are plotted in Fig.19. An acceptable agreement is achieved thus validating the simulations.

Table 2 summarizes the performance of 9 state-of-the-art MIMO antenna design. The designs reported in [31], [32] exhibit higher port-to-port isolation than the proposed antenna. However, their diversity gain, ECC, and efficiency were not reported. In summary the proposed MIMO antenna offers high efficiency, good port-to-port isolation, and high diversity gain. It also benefits from having a low cost planar structure as well as a versatile design which can be altered to the gain or numbers of elements.

IV. CONCLUSION

Multiple input multiple output (MIMO) antennas with pattern diversity are a key technology for modern mobile communication system which enable high spectral efficiency. A key limiting factor in this technology is the size of the device which limits the number of radiating elements. This is due to the fact that preserving high isolation between radiating elements installed within a limited volume of space is a challenging task. This paper presents a technique for MIMO antenna design that can be used to integrate any number of antenna elements on to a common ground plane. Using this technique ensures the high isolation between the ports and

can lead to directive patterns from each element in the MIMO antenna. This makes the resulting design suitable for pattern diversity. The technique is applied on a IFA antenna and to test the validity of the proposed technique, 4 and 6 elements MIMO antenna are simulated and fabricated. A good agreement between the simulation and measurement is achieved which can validates the proposed technique. This technique can be a good candidate to design massive MIMO antenna for the 5G system where large number of antennas in a limited space is required.

REFERENCES

[1] J. Malik, A. Patnaik, and M. Kartikeyan, "Novel printed MIMO antenna with pattern and polarization diversity," *IEEE Antennas Wireless Propag. Lett.*, vol. 14, pp. 739–742, 2015.
[2] D. Sarkar, K. Saurav, and K. V. Srivastava, "Dual band complementary split-ring resonator-loaded printed dipole antenna arrays for pattern diversity multiple-input–multiple-output applications," *IET Microw., Antennas Propag.*, vol. 10, no. 10, pp. 1113–1123, 2016.
[3] J. Malik, D. Nagpal, and M. V. Kartikeyan, "Mimo antenna with omnidirectional pattern diversity," *Electron. Lett.*, vol. 52, no. 2, pp. 102–104, 2016.
[4] D. Sarkar, A. Singh, K. Saurav, and K. V. Srivastava, "Four-element quad-band multiple-input–multiple-output antenna employing split-ring resonator and inter-digital capacitor," *IET Microw., Antennas Propag.*, vol. 9, no. 13, pp. 1453–1460, 2015.
[5] Z. Qin, G.-Y. Wen, M. Zhang, and J. Wang, "Printed eight-element MIMO system for compact and thin 5G mobile handest," *Electron. Lett.*, vol. 52, no. 6, pp. 416–418, Mar. 2016.
[6] Y. Pan, Y. Cui, and R. Li, "Investigation of a triple-band multibeam MIMO antenna for wireless access points," *IEEE Trans. Antennas Propag.*, vol. 64, no. 4, pp. 1234–1241, Apr. 2016.
[7] E. Yetisir, C.-C. Chen, and J. L. Volakis, "Wideband low profile multiport antenna with omnidirectional pattern and high isolation," *IEEE Trans. Antennas Propag.*, vol. 64, no. 9, pp. 3777–3786, Sep. 2016.
[8] D. Sarkar, K. Saurav, and K. V. Srivastava, "A compact dual band four element MIMO antenna for pattern diversity applications," in *Proc. IEEE 5th Asia–Pacific Conf. Antennas Propag. (APCAP)*, Jul. 2016, pp. 273–274.
[9] Y. Yang, Q. Chu, and C. Mao, "Multiband mimo antenna for GSM, DCS, and LTE indoor applications," *IEEE Antennas Wireless Propag. Lett.*, vol. 15, pp. 1573–1576, 2016.
[10] L. Sun, W. Huang, B. Sun, Q. Sun, and J. Fan, "Two-port pattern diversity antenna for 3G and 4G MIMO indoor applications," *IEEE Antennas Wireless Propag. Lett.*, vol. 13, pp. 1573–1576, 2014.
[11] A. Toktas and A. Akdagli, "Compact multiple-input multiple-output antenna with low correlation for ultra-wide-band applications," *IET Microw., Antennas Propag.*, vol. 9, no. 8, pp. 822–829, May 2015.
[12] L. Liu, S. W. Cheung, and T. I. Yuk, "Compact MIMO Antenna for portable devices in UWB applications," *IEEE Trans. Antennas Propag.*, vol. 61, no. 8, pp. 4257–4264, Aug. 2013.
[13] H. Wang, L. Liu, Z. Zhang, Y. Li, and Z. Feng, "Ultra-compact three-port MIMO antenna with high isolation and directional radiation patterns," *IEEE Antennas Wireless Propag. Lett.*, vol. 13, pp. 1545–1548, 2014.
[14] S. Ghosh, T.-N. Tran, and T. Le-Ngoc, "Miniaturized four-element diversity PIFA," *IEEE Antennas Wireless Propag. Lett.*, vol. 12, pp. 396–400, 2013.
[15] Y. Yao, X. Wang, X. Chen, J. Yu, and S. Liu, "Novel diversity/MIMO PIFA antenna with broadband circular polarization for multimode satellite navigation," *IEEE Antennas Wireless Propag. Lett.*, vol. 11, pp. 65–68, 2012.
[16] H. Wang, Z. Zhang, and Z. Feng, "Dual-port planar MIMO antenna with ultra-high isolation and orthogonal radiation patterns," *Electron. Lett.*, vol. 51, no. 1, pp. 7–8, 2015.
[17] S. A. Ja'afreh, Y. Huang, and L. Xing, "Low profile and wideband planar inverted-F antenna with polarisation and pattern diversities," *IET Microw., Antennas Propag.*, vol. 10, no. 2, pp. 152–161, 2016.
[18] Y. Gao, X. Chen, Z. Ying, and C. Parini, "Design and performance investigation of a dual-element PIFA array at 2.5 GHz for MIMO terminal," *IEEE Trans. Antennas Propag.*, vol. 55, no. 12, pp. 3433–3441, Dec. 2007.
[19] A. T. M. Sayem, S. Khan, and M. Ali, "A miniature spiral diversity antenna system with high overall gain coverage and low SAR," *IEEE Antennas Wireless Propag. Lett.*, vol. 8, pp. 49–52, 2009.
[20] Y. Ding, Z. Du, K. Gong, and Z. Feng, "A four-element antenna system for mobile phones," *IEEE Antennas Wireless Propag. Lett.*, vol. 6, pp. 655–658, 2007.
[21] H. Li, J. Xiong, and S. He, "A compact planar MIMO antenna system of four elements with similar radiation characteristics and isolation structure," *IEEE Antennas Wireless Propag. Lett.*, vol. 8, pp. 1107–1110, 2009.
[22] C.-Y. Chiu and R. D. Murch, "Compact four-port antenna suitable for portable MIMO devices," *IEEE Antennas Wireless Propag. Lett.*, vol. 7, pp. 142–144, 2008.
[23] H. T. Chattha, M. Nasir, Q. H. Abbasi, Y. Huang, and S. S. AlJa'afreh, "Compact low-profile dual-port single wideband planar inverted-F MIMO antenna," *IEEE Antennas Wireless Propag. Lett.*, vol. 12, pp. 1673–1675, 2013.
[24] T. Wirth, L. Thiele, M. Kurras, M. Mehlhose, and T. Haustein, "Massive MIMO proof-of-concept: Emulations and hardware-field trials at 3.5 GHz," in *Proc. 50th Asilomar Conf. Signals, Syst. Comput.*, Nov. 2016, pp. 1793–1798.
[25] C. Rowell and E. Y. Lam, "Mobile-phone antenna design," *IEEE Antennas Propag. Mag.*, vol. 54, no. 4, pp. 14–34, Aug. 2012.
[26] Q. Rao and D. Wang, "A compact dual-port diversity antenna for long-term evolution handheld devices," *IEEE Trans Veh. Technol.*, vol. 59, no. 3, pp. 1319–1329, Mar. 2010.
[27] Q. Rao and D. Wang, "A compact dual-port diversity antenna for handheld devices," in *Proc. Loughborough Antennas Propag. Conf. (LAPC)*, Nov. 2009, pp. 181–184.
[28] K. Saurav, N. K. Mallat, and Y. M. M. Antar, "A three-port polarization and pattern diversity ring antenna," *IEEE Antennas Wireless Propag. Lett.*, vol. 17, no. 7, pp. 1324–1328, Jul. 2018.
[29] D.-W. Kim and S. Nam, "Systematic design of a multiport MIMO antenna with bilateral symmetry based on characteristic mode analysis," *IEEE Trans. Antennas Propag.*, vol. 66, no. 3, pp. 1076–1085, Mar. 2018.
[30] Y. Gao, R. Ma, Y. Wang, Q. Zhang, and C. Parini, "Stacked patch antenna with dual-polarization and low mutual coupling for massive MIMO," *IEEE Trans. Antennas Propag.*, vol. 64, no. 10, pp. 4544–4549, Oct. 2016.
[31] Y. Tawk, J. Costantine, and C. G. Christodoulou, "An eight-element reconfigurable diversity dipole system," *IEEE Trans. Antennas Propag.*, vol. 66, no. 2, pp. 572–581, Feb. 2018.
[32] D. Sarkar and K. V. Srivastava, "A compact four-element MIMO/diversity antenna with enhanced bandwidth," *IEEE Antennas Wireless Propag. Lett.*, vol. 16, pp. 2469–2472, 2017.
[33] A. Boukarkar, X. Q. Lin, Y. Jiang, L. Y. Nie, P. Mei, and Y. Yu, "A miniaturized extremely close-spaced four-element dual-band MIMO antenna system with polarization and pattern diversity," *IEEE Antennas Wireless Propag. Lett.*, vol. 17, no. 1, pp. 134–137, Jan. 2018.
[34] R. Chandel, A. K. Gautam, and K. Rambabu, "Tapered fed compact UWB MIMO-diversity antenna with dual band-notched characteristics," *IEEE Trans. Antennas Propag.*, vol. 66, no. 4, pp. 1677–1684, Apr. 2018.
[35] Y. Sharma, D. Sarkar, K. Saurav, and K. Srivastava, "Three-element MIMO antenna system with pattern and polarization diversity for WLAN applications," *IEEE Antennas Wireless Propag. Lett.*, vol. 16, pp. 1163–1166, 2017.
[36] X. Zhao, S. P. Yeo, and L. C. Ong, "Planar UWB MIMO antenna with pattern diversity and isolation improvement for mobile platform based on the theory of characteristic modes," *IEEE Trans. Antennas Propag.*, vol. 66, no. 1, pp. 420–425, Jan. 2018.

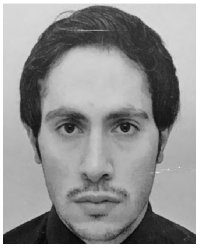

YASIN KABIRI received the M.Eng. degree (Hons.) in electronics and communication engineering from the University of Birmingham, Birmingham, U.K., in 2012, and the Ph.D. degree from the School of Electronic and Electrical Engineering, University of Birmingham, in 2015. During his Ph.D. degree, he has developed an approach called Injection Matching Theory (IMT) that can be used for making small, wide band, and reconfigurable antennas with high efficiency. He is currently a Research Fellow with the 5G Innovation Centre, where he was involved in 5G antennas. His current research interests include the areas of RF and microwave, electrically small antenna, reconfigurable antennas, active antennas, microwave filters, and broadband and multiband antennas.

ALEJANDRO L. BORJA received the M.Sc. degree in telecommunication engineering and the Ph.D. degree from the Universitat Politécnica de Valéncia, Valencia, Spain, in 2004 and 2009, respectively. From 2005 to 2006, he was with the University of Birmingham, Birmingham, U.K. From 2007 to 2008, he was with the Universite de Lille 1, Lille, France. Since 2009, he has been with the Universidad de Castilla-La Mancha, Spain, where he is currently an Assistant Lecturer. He has published more than 50 papers in peer-reviewed international journals and conference proceedings. His research interests include EM metamaterials, substrate integrate waveguide, and reconfigurable devices and their applications in microwave and millimetric bands. He was a recipient of the 2008 CST Short Paper Award. He frequently acts as a Reviewer for several technical publications.

JAMES R. KELLY (M'10) received the master's degree in electronic and electrical engineering and the Ph.D. degree in microwave filters from Loughborough University, U.K., in 2002 and 2007, respectively. From 2001 to 2012, he was with the Rolls-Royce Strategic Research Centre and Airbus Defence and Space, Ltd. From 2007 to 2012, he was a Research Fellow/Associate with Loughborough University and the Universities of Birmingham, Durham, and Sheffield. In 2009, he launched a small company that provides technical training on microwave antenna design (microwave and RF solutions). From 2012 to 2013, he was a Lecturer with Anglia Ruskin University, Cambridge, U.K. In 2013, he joined the Institute for Communication Systems (ICS), University of Surrey, U.K., where he is currently a Lecturer in microwave antennas. He also has experience of working on small antennas for portable device applications, UWB antennas, planar microwave filters, metamaterials, and material characterization. He has published almost 80 academic papers in peer-reviewed journals and conference proceedings. He holds a European patent on reconfigurable antennas. His research interest includes reconfigurable antennas. He is a member of the Institution of Engineering and Technology (IET), the Institute of Electrical and Electronics Engineers (IEEE), and the IEEE Industrial Electronics Society.

PEI XIAO (SM'11) was with Newcastle University and Queen's University Belfast. He also held positions at Nokia Networks in Finland. He is currently a Professor with the Home of 5G Innovation Centre (5GIC), Institute for Communication Systems, University of Surrey. He is also the Technical Manager of 5GIC, leading the research team on the new physical layer work area and coordinating/supervising research activities across all the working areas within 5GIC. He has published extensively in the fields of communication theory and signal processing for wireless communications.